

PRIN 2022 PNRR Call for Proposals (D.D.1409 of 14/09/2022)

AIMS

Artificial Intelligence to Monitor our Seas

Project number: P2022587FM

Starting date: 30th November 2023 – Duration: 24 months

Deliverable D2.5

Report on Second Gate clearance of AI algorithms

**DOCUMENT INFORMATION**

Deliverable number	D2.5
Deliverable title	Buoys layout simulation for reconstruction algorithms
Work Package	WP2
Deliverable type¹	R
Dissemination level²	P
Due date	31.05.2025 (Month 18)
Pages	22
Document version³	2.0
Lead author(s)	Leonardo Gambarelli, Edoardo Pasta (POLITO)
Contributors	Giuseppe Giorgi (POLITO)

AIMS: Artificial Intelligence to Monitor our Seas is funded by the European Union – NextGeneration EU within the PRIN 2022 PNRR program (D.D.1409 del 14/09/2022 Ministero dell'Università e della Ricerca). This document reflects only the authors' view, and the Commission and Ministry cannot be considered responsible for any use that may be made of the information it contains.

1 Type: R: Report; D: Dataset

2 Dissemination level: C: Confidential; P: Public

3 First digit: 0: draft; 1: peer review; 2: peer review 3: coordinator approval; 4: final version





DOCUMENT CHANGE HISTORY

Version	Date	Author		Description
DRAFT				
0.1	10.05.2025	Leonardo (POLITO)	Gambarelli	Creation
FIRST PEER REVIEW				
1.0	20.05.2025	Edoardo (POLITO)	Pasta	Consolidation of input from reviewers
FINAL VERSION				
2.0	31.05.2025	Giuseppe (POLITO)	Giorgi	Final and formal review, version ready for submission





SHORT ABSTRACT FOR DISSEMINATION PURPOSES

Abstract

This deliverable continues the previous first-gate clearance (D2.2) by further testing the algorithms at reconstructing H_s and T_p simulating different possible buoys disposition layouts. Three training layouts—grid, random, and perpendicular lines— have been chosen within a fixed area and common validation over multiple snapshots. We compare the achieved Mean Absolute Error for all the algorithms and all the training setups. Grid training consistently gives the lowest error, with random disposition performing the best, while the perpendicular lines setup performs the worst. From the obtained results, GPR seems to be the most reliable algorithm.





TABLE OF CONTENTS

1. Introduction	10
1.1 Experiment description	10
2. Training points/buoys layout definition	12
2.1 Grid-like points layout.....	12
2.2 Perpendicular lines points layout.....	12
2.3 Random points layout	13
3. Validation points disposition	15
4. Results.....	16
5. Conclusions	21
REFERENCES	22





LIST OF PARTNERS

N°	Logo	Name	Short Name	City
1	 Politecnico di Torino	Politecnico di Torino	POLITO	Torino
2	 ROMA TRE UNIVERSITÀ DEGLI STUDI	Università degli studi di Roma Tre	ROMA3	Roma
3	 Italian National Research Council	Consiglio Nazionale delle Ricerche	CNR	Firenze





ABBREVIATIONS

Acronym	Description
ANN	Artificial Neural Network
GPR	Gaussian Process Regression
MAE	Mean Absolute Error
RBF	Radial Basis Function
RF	Random Forest
TPS	Thin Plate Spline





LIST OF FIGURES

Figure 1 - Disposition of the grid-like points layout.	12
Figure 2 - Disposition of the perpendicular lines points layout.	13
Figure 3 - Disposition of the random points layout.	14
Figure 4 - Disposition of the validation points.	15
Figure 5 - Obtained MAE for Hs reconstruction with grid-like training setup	16
Figure 6 - Obtained MAE for Tp reconstruction with grid-like training setup	16
Figure 7 - Obtained MAE for Hs reconstruction with perpendicular lines training setup.	17
Figure 8 - Obtained MAE for Tp reconstruction with perpendicular lines setup.	17
Figure 9 - Obtained MAE for Hs reconstruction with random points training setup.	18
Figure 10 - Obtained MAE for Tp reconstruction with random points training setup.	18

LIST OF TABLES

Table 1 - Average MAE achieved by the reconstruction algorithms with grid-like points training setup.	19
Table 2 - Average MAE achieved by the reconstruction algorithms with perpendicular lines points training setup.	19
Table 3 - Average MAE achieved by the reconstruction algorithms with random points training setup.	19





EXECUTIVE SUMMARY

This deliverable extends D2.2 by stress-testing five interpolation approaches—Thin-Plate Spline (TPS), Radial Basis Function (RBF), Gaussian Process Regression (GPR), Random Forest (RF), and a shallow feed-forward ANN—for reconstructing significant wave height (H_s) and peak period (T_p) from sparse in-situ observations.

We simulated three alternative deployment layouts of nine buoys within the target area: a 3×3 grid, two perpendicular lines crossing at the center, and nine random points uniformly sampled inside the same rectangle. For each layout and for each parameter (H_s , T_p), we trained on the nine buoy locations (inputs: latitude/longitude; output: the parameter value) and evaluated on a common set of 50 validation points. The experiment was repeated over 50 temporal snapshots from 2022, yielding a consistent, cross-algorithm comparison. Performance was measured with mean absolute error (MAE), computed per snapshot and then aggregated by layout and parameter.

Results are clear and stable across both H_s and T_p : the grid layout consistently delivers the lowest MAE, the random layout performs closely behind, and the perpendicular-lines layout is the weakest. Among the tested methods, GPR emerges as the most reliable overall on these settings, with the other techniques trailing by small but persistent margins depending on the parameter and layout. These findings support grid-like planning for sparse buoy deployments and favor GPR as a robust default interpolator for operational reconstructions, with random layouts as a viable fallback when grid placements are impractical.





1. Introduction

This deliverable aims at continuing the first gate clearance report D2.2 [1] by further testing the algorithms that passed that gate.

The candidate methods are:

- Thin-Plate Spline (TPS)
- Radial Basis Functions (RBF)
- Gaussian Process Regression (GPR)
- Random Forest (RF)
- Artificial Neural Networks (ANN)

1.1 Experiment description

We use the numerical dataset from D1.1 [2], previously adopted in D2.2. Each method estimates Significant Wave Height (H_s) and Peak Period (T_p) from a small set of spatially sparse observations, which are fixed in space for each setup, simulating a possible buoys layout disposition.

Following the protocol adopted in D2.2, the reconstruction task is confined strictly to the spatial domain. Each temporal acquisition (i.e., each snapshot) is processed as an autonomous realization of the field and handled in complete isolation from all others; accordingly, no inter-temporal dependence, memory effect, or autoregressive structure is modelled, exploited, or even assumed to exist.

We randomly selected 50 temporal snapshots from the 2022 record and, for each such instant, extracted the corresponding SWAN fields from the D1.1 dataset. For every one of these 50 snapshots—and for each of the two target parameters (H_s and T_p)—we assembled four companion datasets: three distinct training sets, obtained by subsampling according to the three buoy-deployment layouts (grid, perpendicular lines, random), and a single validation set held in common across layouts to guarantee strict comparability. In this way, each algorithm was exercised over 50 independent test episodes for every (training-layout, parameter) pairing, yielding a balanced and repeatable benchmarking design. Finally, to preclude artefacts due to coastlines/land cells and to avoid geometric infeasibilities in hypothetical buoy placement, we restricted the analysis to the central subdomain of the numerical grid—i.e., the open-water core region of the simulation.





For each experimental configuration, model skill was quantified via the Mean Absolute Error (MAE) computed exclusively at the validation points by averaging, over that set, the absolute differences between the reconstructed values and the reference fields for the same snapshots.

$$MAE = \frac{1}{T} \sum_{i=1}^T |z_i - \hat{z}_i|$$



2. Training points/buoys layout definition

We confined the analysis to a geographical subdomain delimited by latitudes 43.0° – 43.6° N and longitudes 9.5° – 10.1° E. Within this window, we specified three alternative buoy-deployment layouts, which provided the training locations for all interpolation algorithms, and we separately selected a set of validation points—distinct from the training sites—used exclusively to assess the quality of the reconstructed fields. The number of training points was fixed to 9 for all setup, simulating 3 different ways of arranging 9 buoys in the considered area.

2.1 Grid-like points layout

The first training configuration adopts a regular 3×3 lattice inscribed within the selected subdomain, whose four outermost nodes are anchored to the domain's bounding corners—i.e., the grid spans the area from edge to edge, with its vertices coincident with the extremes of the considered zone.

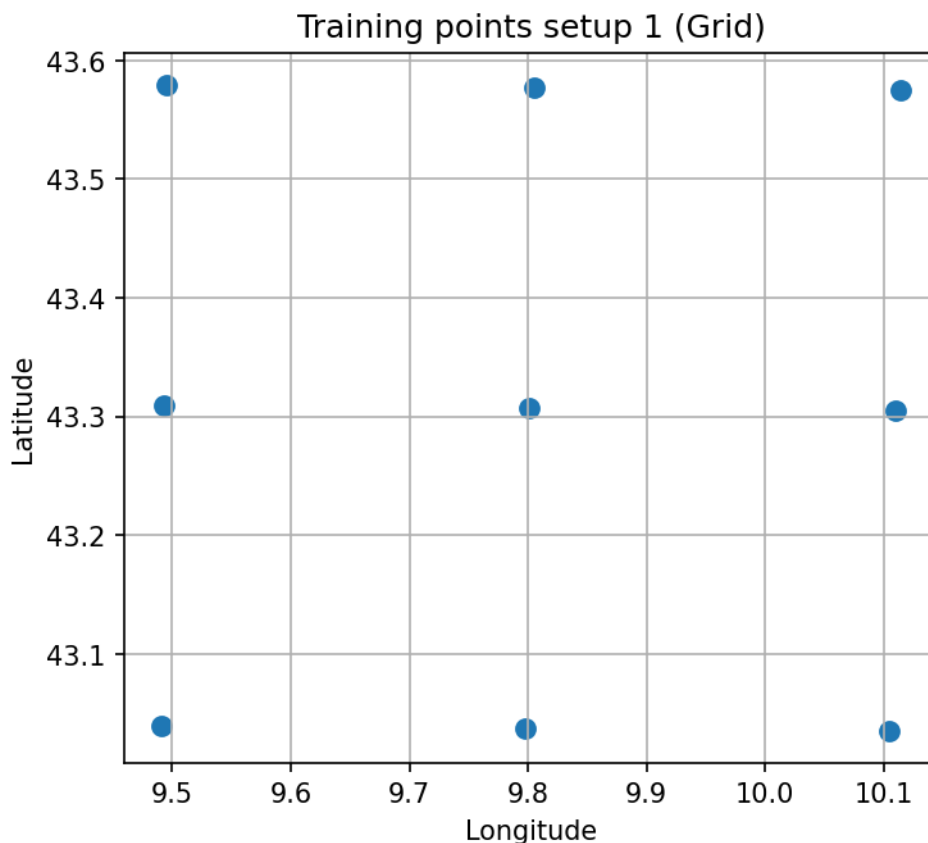


Figure 1 – Disposition of the grid-like points layout.

2.2 Perpendicular lines points layout



The second training configuration is defined by two mutually perpendicular alignments of buoy sites—one arranged along a constant latitude (zonal, east–west) and the other along a constant longitude (meridional, north–south)—which intersect at the geometric center of the analysis domain.

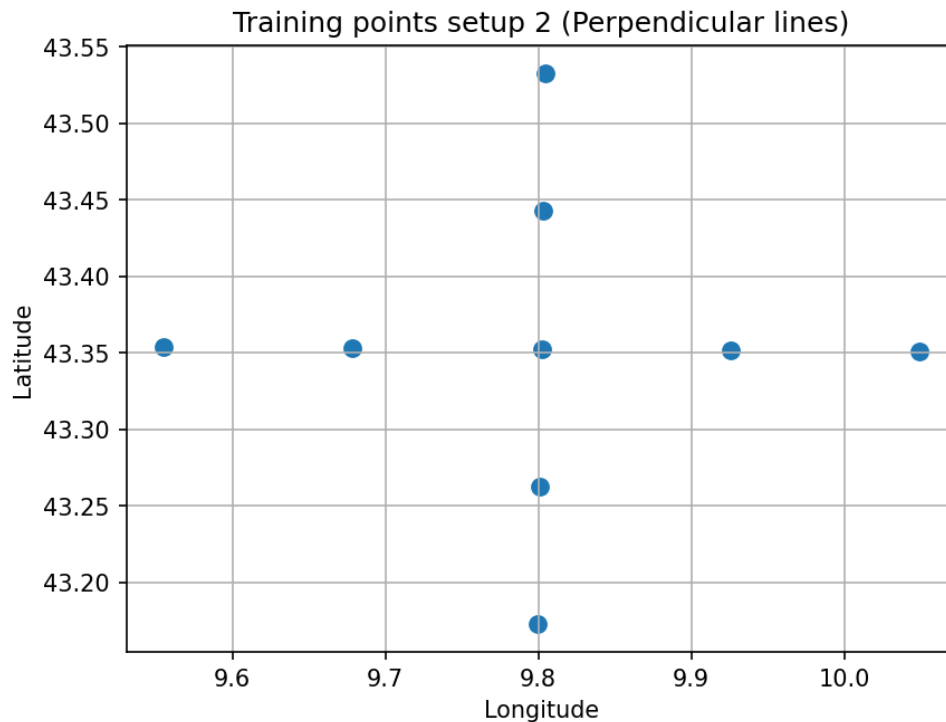


Figure 2 – Disposition of the perpendicular lines points layout.

2.3 Random points layout

The third and final training configuration comprises nine buoy locations randomly sampled from within the bounds of the designated study area—selected without imposing any geometric regularity beyond inclusion in the admissible subdomain—thereby yielding an unstructured, uniformly drawn layout representative of a purely stochastic placement.



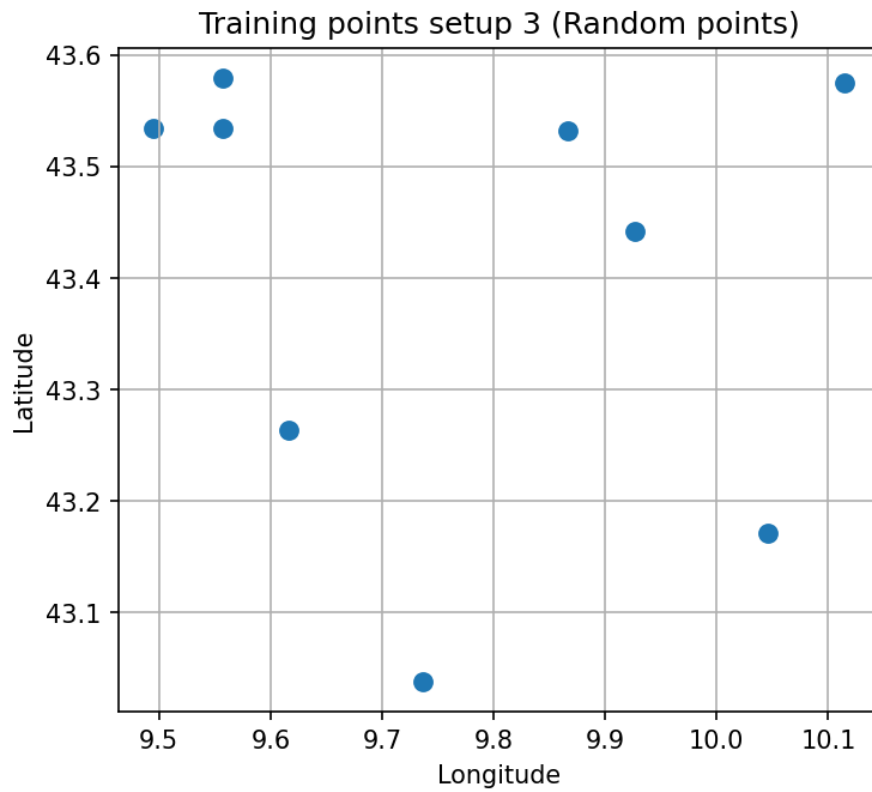


Figure 3 – Disposition of the random points layout.





3. Validation points disposition

To secure an unbiased appraisal of algorithmic performance, each reconstruction was evaluated on a held-out set of 50 validation locations drawn from within the same geographic window. These validation points were randomly sampled subject to a single, stringent exclusion criterion: any candidate coinciding with a training site in *any* of the three buoy-layout configurations was rejected and resampled. This procedure ensures that the validation set is strictly disjoint from all training layouts, thereby preventing leakage, preserving statistical independence between training and testing, and yielding an impartial estimate of reconstruction accuracy.

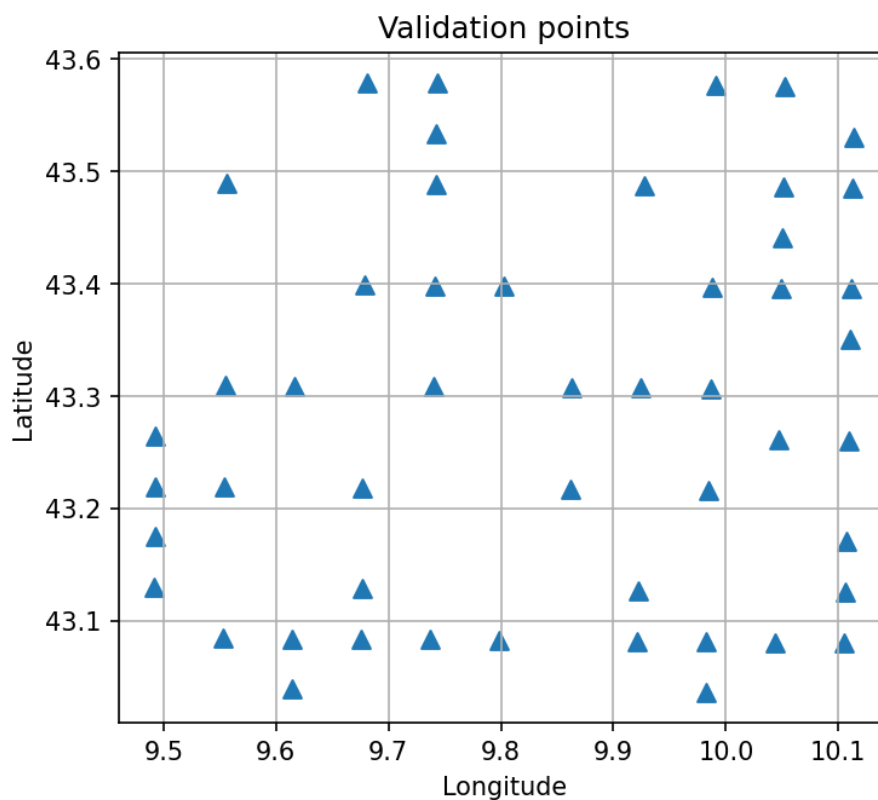


Figure 4 – Disposition of the validation points.





4. Results.

The figures and the tables below report the obtained MAE for each algorithm, divided by training points layout used and parameter reconstructed.

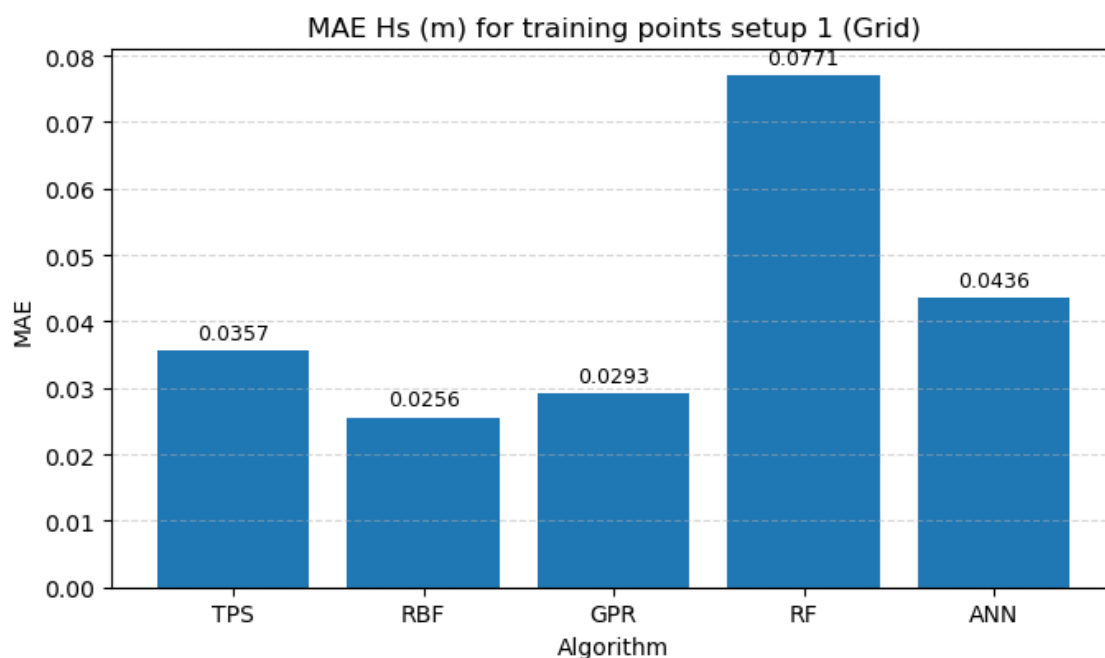


Figure 5 – Obtained MAE for Hs reconstruction with grid-like training setup

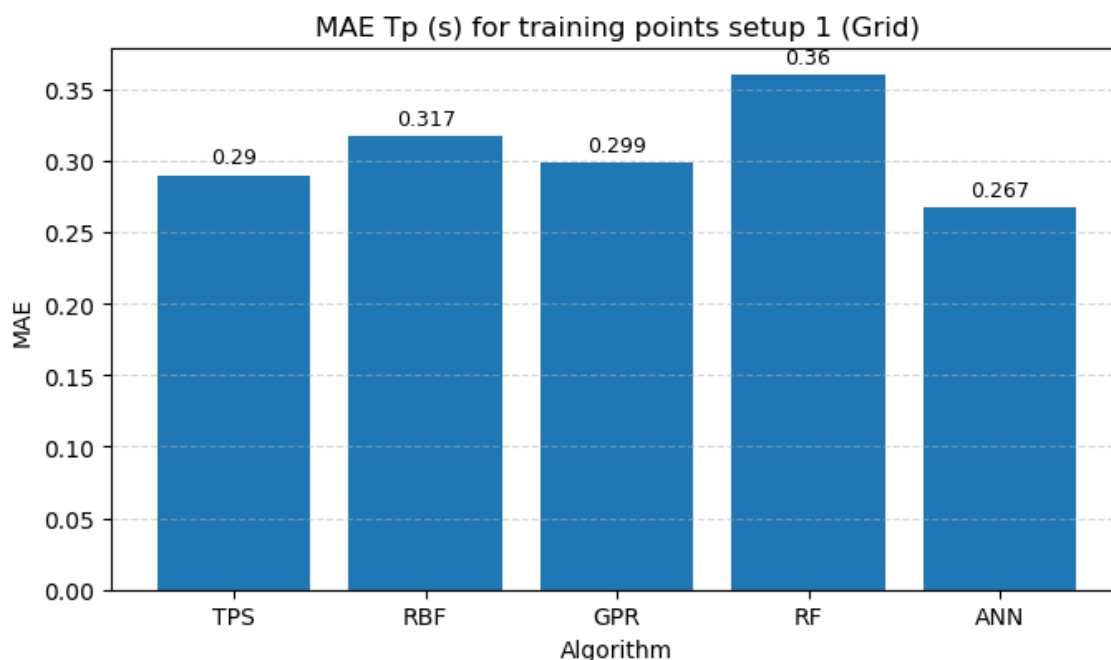


Figure 6 – Obtained MAE for Tp reconstruction with grid-like training setup



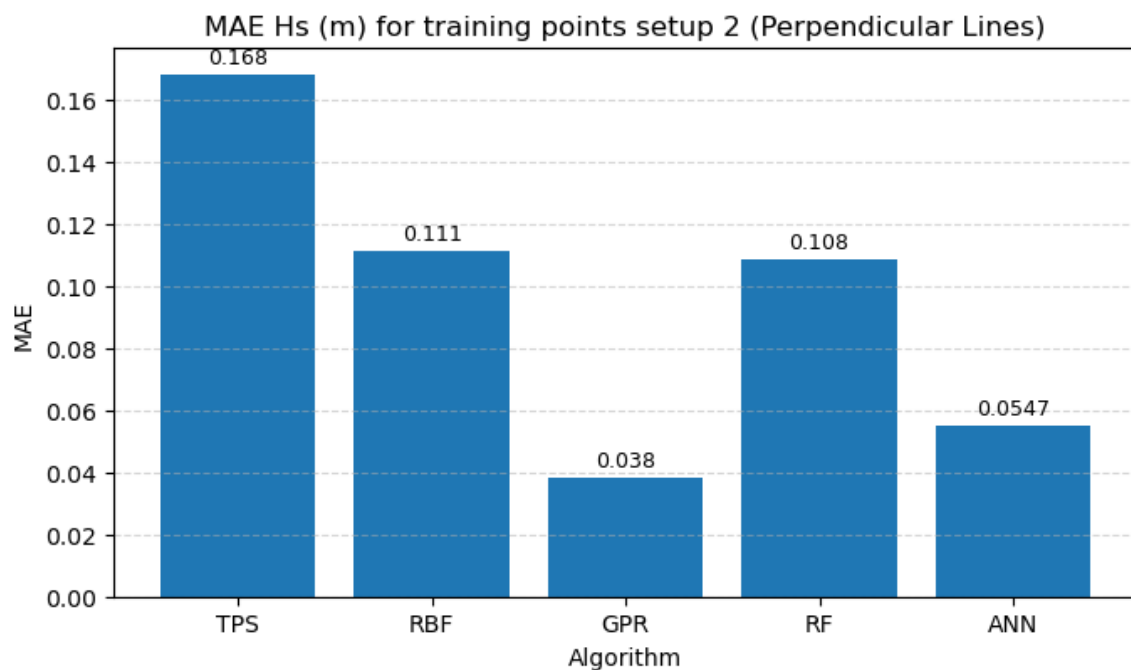


Figure 7 – Obtained MAE for Hs reconstruction with perpendicular lines training setup

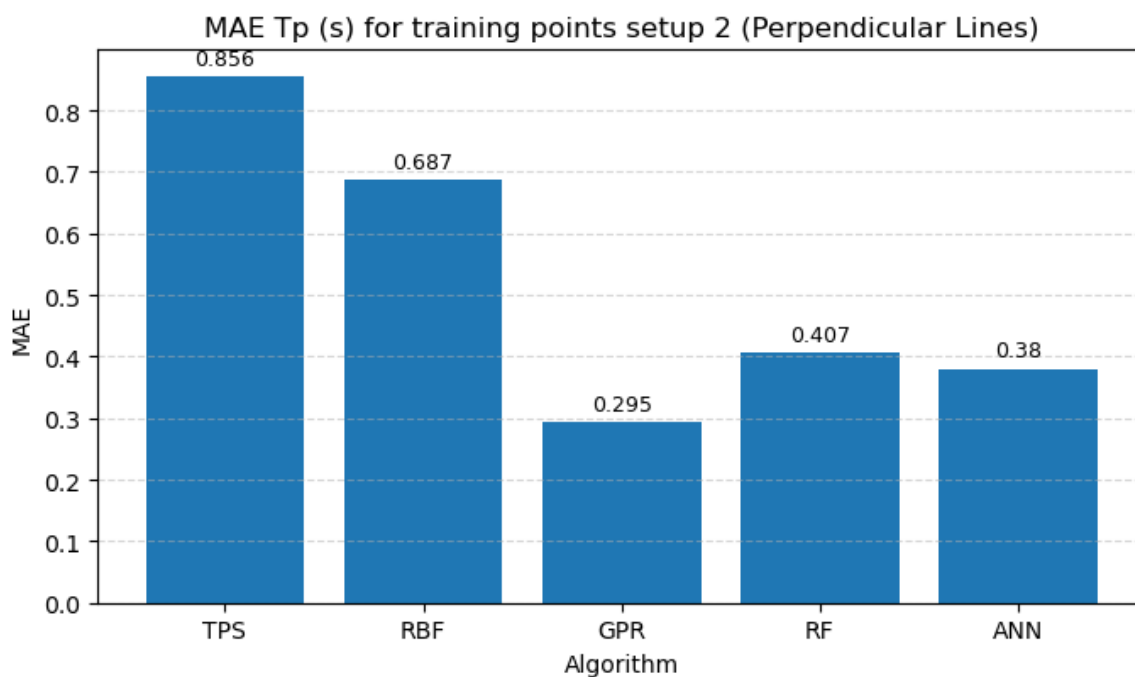


Figure 8 – Obtained MAE for Tp reconstruction with perpendicular lines setup



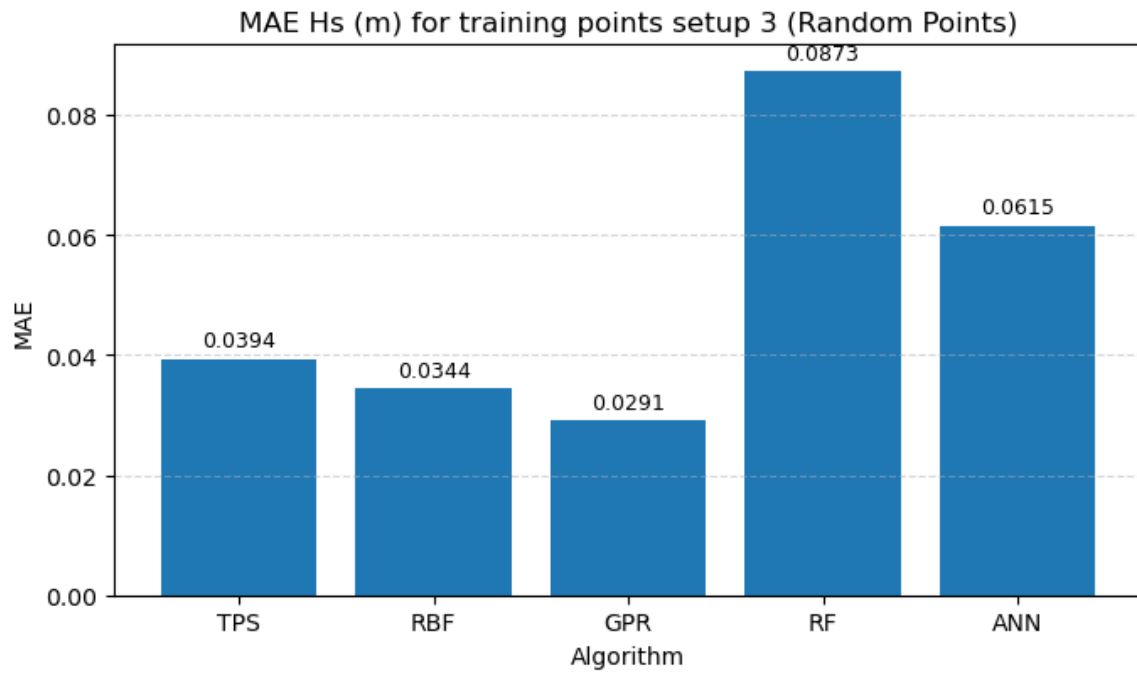


Figure 9 – Obtained MAE for Hs reconstruction with random points training setup

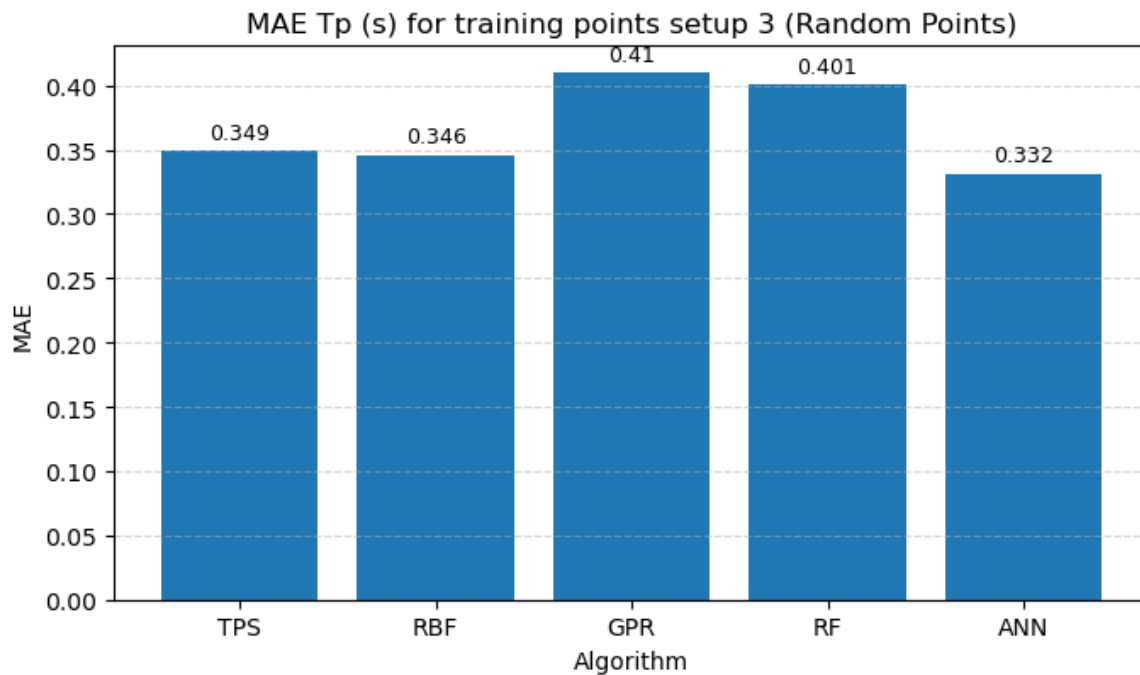


Figure 10 – Obtained MAE for Tp reconstruction with random points training setup



**Table 1 – Average MAE achieved by the reconstruction algorithms with grid-like points training setup.**

Algorithm	Hs (m)	Tp(s)
TPS	0.0357 m	0.29 s
RBF	0.0256 m	0.317 s
GPR	0.0293 m	0.299 s
RF	0.0771 m	0.36 s
ANN	0.0436 m	0.267 s

Table 2 – Average MAE achieved by the reconstruction algorithms with perpendicular lines points training setup.

Algorithm	Hs (m)	Tp (s)
TPS	0.168 m	0.856
RBF	0.111 m	0.687
GPR	0.038 m	0.295
RF	0.108 m	0.407 s
ANN	0.0547 m	0.38 s

Table 3 – Average MAE achieved by the reconstruction algorithms with random points training setup.

Algorithm	Hs (m)	Tp (s)
TPS	0.0394 m	0.349 s
RBF	0.0344 m	0.346 s
GPR	0.0291 m	0.41 s
RF	0.0873 m	0.401 s
ANN	0.0615 m	0.332 s

A careful inspection of the accompanying figures and tables reveals a stable, cross-method pattern: across virtually all algorithms, reconstruction errors are systematically lower under the grid-like and random-points layouts than under the perpendicular-lines configuration. Between the two stronger layouts, the regular 3×3 grid confers a small but persistent advantage over random sampling, indicating that quasi-uniform two-dimensional coverage yields benefits beyond mere sample count. A further, noteworthy exception concerns GPR: uniquely among the tested methods, its performance deteriorates only mildly on the perpendicular-lines layout, evidencing a relative robustness to anisotropic, non-uniform training





geometries and an ability to recover the target fields even when spatial sampling collapses toward one-dimensional transects.





5. Conclusions

This deliverable assessed five interpolation/regression methods (TPS, RBF, GPR, RF, ANN) for reconstructing H_s and T_p from sparse observations, using three alternative training-point layouts (3×3 grid, perpendicular lines, random) within a fixed subdomain and 50 held-out validation points per snapshot. Experiments were run on 50 snapshots from 2022, treating each time slice independently (purely spatial inference), and performance was measured by MAE computed at validation locations.

Across layouts and parameters, a consistent pattern emerged. The grid layout delivered the lowest errors, the random layout performed close to grid, and the perpendicular-lines layout was consistently worst—indicating that broad, quasi-uniform 2-D coverage is far more informative than one-dimensional spanning. This trend is visible throughout the figures and summarized tables included in the report. Regarding algorithms, GPR stood out as the most reliable overall, in particular showing notable robustness under the perpendicular-lines layout where other methods deteriorated markedly. TPS and RBF remained competitive under grid/random layouts (with ANN occasionally strongest on T_p in those cases), while RF trailed in most settings with these very small training sets. These method-specific behaviors, together with the layout effects, are reflected in the comparative MAE tables for each configuration.

For operational deployments or planning of in situ sampling, it is recommended to prioritize a grid-like buoy disposition whenever feasible; where logistics preclude a strict grid, a random/unstructured placement still yields strong performance, provided coverage remains distributed in 2-D. Configurations dominated by perpendicular transects should be avoided unless dictated by constraints, in which case GPR is the preferable interpolator due to its resilience to anisotropic sampling.





REFERENCES

- [1] Deliverable D2.2 Report on the first gate clearance of AI algorithms.
- [2] Deliverable D1.1 Report and dataset from wave models.

